ISSN: 2641-6360
DOI: 10.33552/WJOVR.2025.05.000604
World Journal of Ophthalmology & Vision Research
Iris Publishers

Review Article

An Overview of Pentacam® Indices

Farideh Doroodgar[1,2], MD, FICO, MPH, Maedeh Mazloomi[1,3], MD, Sana Niazi[1,2]*, MD, PhD, MPH, Sepehr Feizi[4], MD, MSc, Mohammad Hasan Shahriari[5], PhD and Amir Faramarzi[4,6], MD

[1]*Negah Aref Ophthalmic Research Center, Shahid Beheshti University of Medical Sciences, Tehran, Iran*

[2]*Translational Ophthalmology Research Center, Tehran University of Medical Sciences, Tehran, Iran*

[3]*School of Medicine, Isfahan University of Medical Sciences, Isfahan, Iran*

[4]*Ophthalmic Research Center, Research Institute for Ophthalmology and Vision Science, Shahid Beheshti University of Medical Sciences, Tehran, Iran*

[5]*Department of Health Information Technology and Management, School of Allied Medical Sciences, Shahid Beheshti University of Medical Sciences, Tehran, Iran*

[6]*Department of Ophthalmology, Morsani College of Medicine, USF Health, Tampa, FL, USA*

***Corresponding author:** Sana Niazi, Negah Aref Ophthalmic Research Center, Shahid Beheshti University of Medical Sciences, Tehran, Iran. Translational Ophthalmology Research Center, Tehran University of Medical Sciences, Tehran, Iran.

Received Date: January 07, 2025
Published Date: January 20, 2025

Abstract

The Pentacam® device utilizes a rotating Scheimpflug camera to precisely measure corneal features such as anterior and posterior elevations, corneal thickness, and topography. Its ersatile, user-friendly nature has made it the subject of numerous in-depth studies. However, given the extensive amount of available data, providing a concise summary of the diagnostic steps for keratoconus (KC) and subclinical keratoconus (SKC) can be challenging. This review aims to provide a clear and succinct overview of Pentacam® and its associated indices (Figure 1. Graphical Abstract: Schematic Presentation). Key metrics, including the Belin-Ambrosio Enhanced Ectasia Display (BAD-D), Ambrósio relational thickness (ART), and Pachymetric Progression Index (PPI), are examined for their diagnostic effectiveness. These indices are highly reliable for identifying clinical KC, though their sensitivity to SKC remains lower, in part due to varied diagnostic criteria in early stages. The Pentacam Random Forest Index (PRFI), while integrating artificial intelligence, also faces challenges in SKC detection. Additionally, the Pentacam®'s role in pre-and post-surgical assessments, such as for refractive surgery, phakic IOL (pIOL) insertion, and less common conditions like pellucid marginal degeneration (PMD) and keratoglobus, is discussed. Despite its limitations, Pentacam® remains essential in early ectasia detection, with future enhancements likely to focus on AI integration and standardized diagnostic methods.

Keywords: Keratoconus; Corneal topography; Pachymetry; Scheimpflug imaging; Pentacam; Tomography, Optical coherence; Diagnostic, Imaging; Cornea

Abbreviations: ACD: Anterior chamber Depth; ACA: Anterior Chamber Angle; ACV: Anterior Chamber Volume; AI: Artificial Intelligence; ART: Ambrósio Relational Thickness; BAD-D: Belin-Ambrosio Enhanced Ectasia Display; BCVA: Best Corrected Distance Visual Acuity; BFS: Best-Fit Sphere; BFTE: Best-Fit Toric Ellipsoid; CCT: Central Corneal Thickness; CKI: Central Keratoconus Index; CTSP: Corneal Thickness Spatial Profile; ECC: Endothelial Cell Count; FFKC: Forme Fruste Keratoconus; IHD: Index of Height Decentration; IHA: Index of Height Asymmetry; IOL: Intraocular Lens; ISV: Index of Surface Variance; IVA: Index of Vertical Asymmetry; KC: Keratoconus; Km: Mean Curvature; LASIK: Laser-Assisted In Situ Keratomileusis; PPI: Pachymetric Progression Index; pIOL: Phakic Intraocular Lens; PMD: Pellucid Marginal Degeneration; PRK: Photorefractive Keratectomy; PRFI: Pentacam Random Forest Index; PTI: Percentage Thickness Increase; ROC: Radius of Curvature; Rmin: Minimal Sagittal Curvature; SKC: Subclinical Keratoconus; TCT: Thinnest Corneal Thickness (summarized in Figure 1. Graphical Abstract).

Schematic presentation of features of Pentacam AXL/ wave (a)

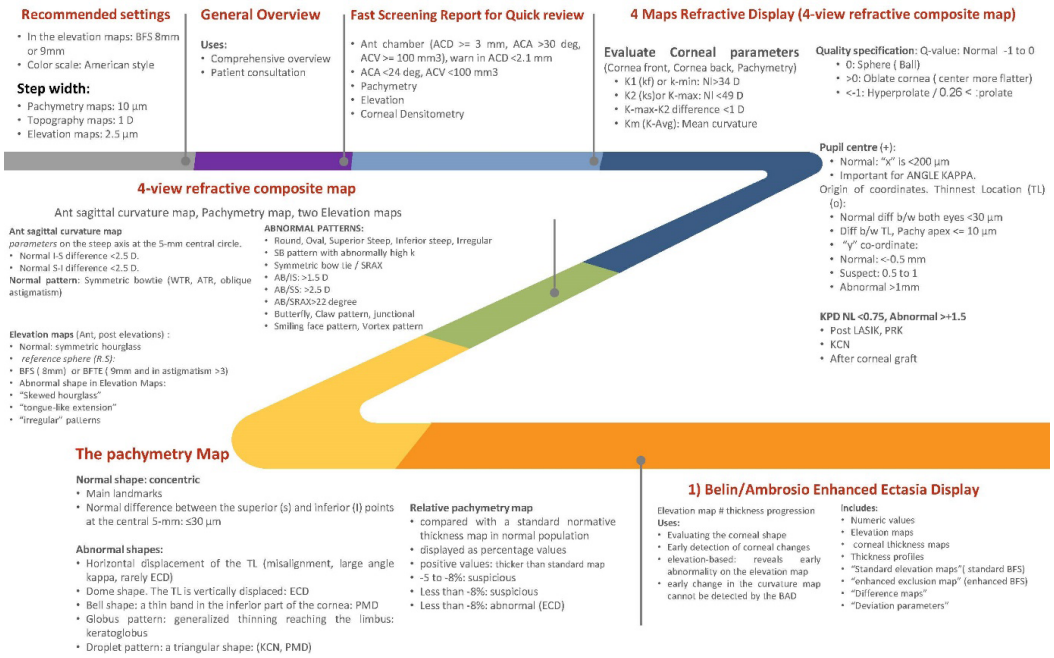

Schematic presentation of features of Pentacam AXL/ wave (b)

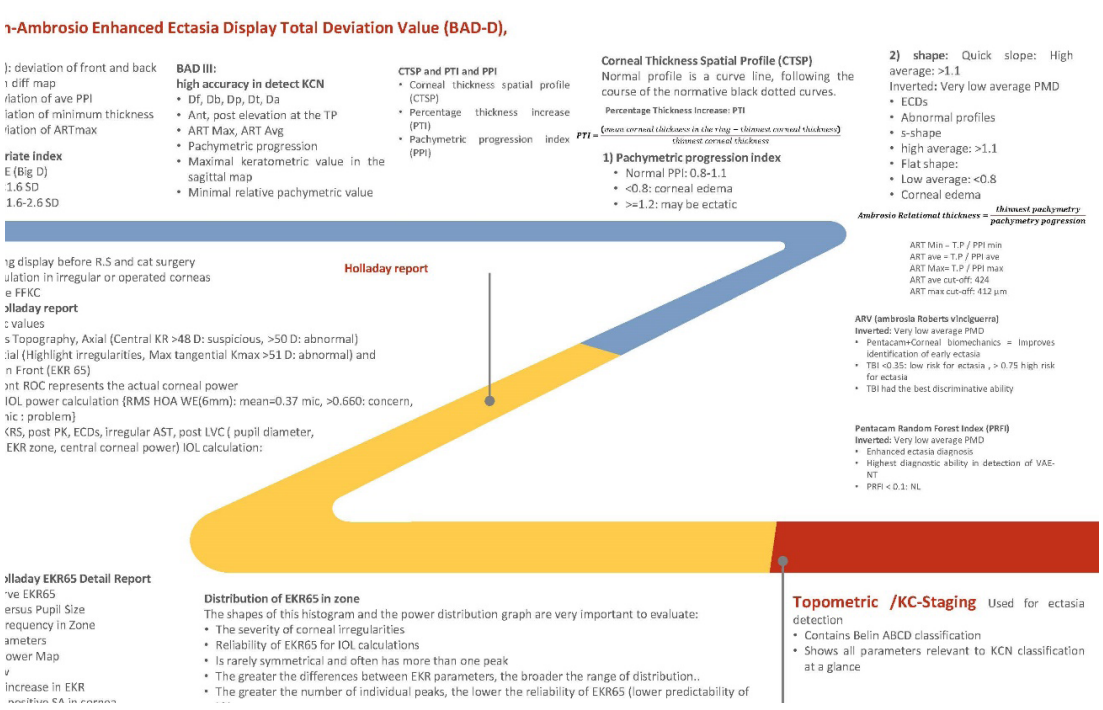

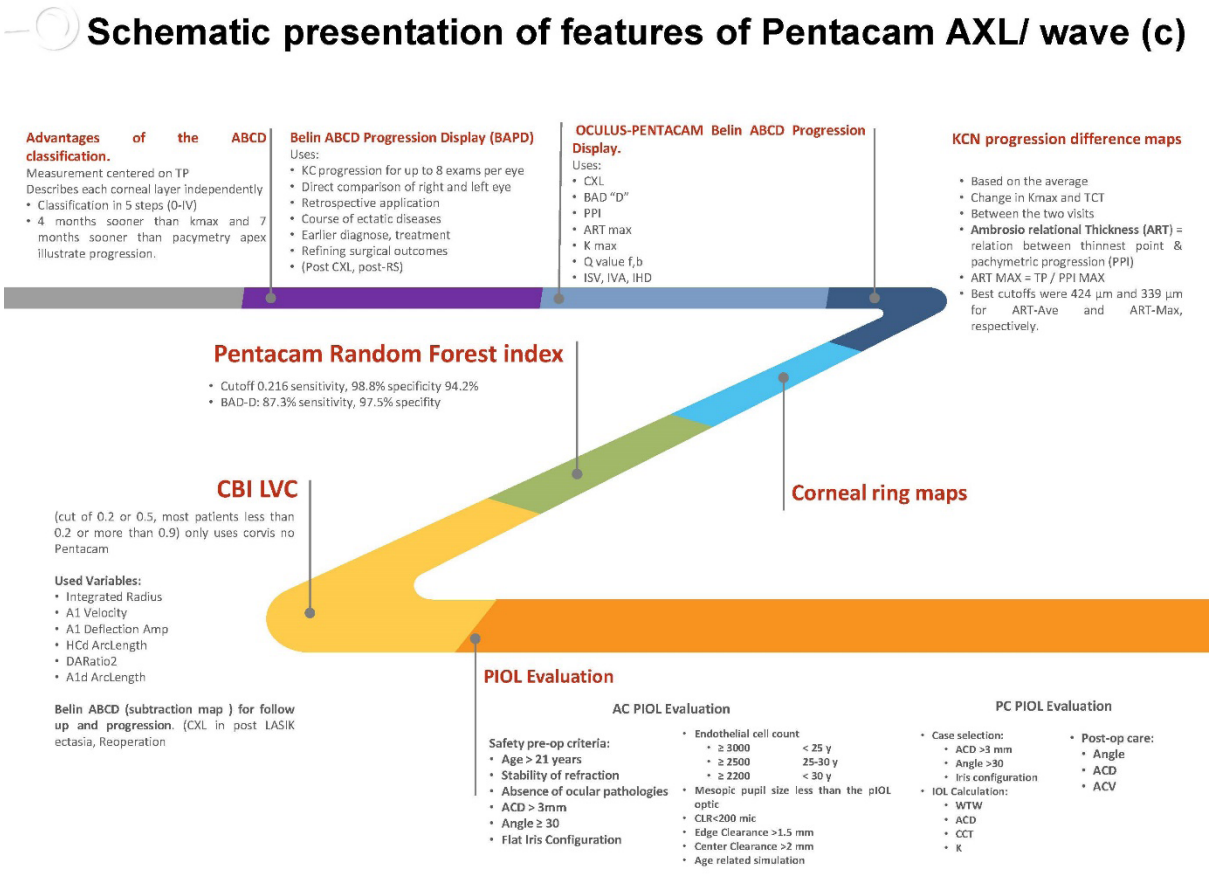

Figure 1.

Introduction

The Pentacam® system employs a rotating Scheimpflug camera, paired with a 14-mm monochromatic slit light system that uses 475-nm blue light diodes to capture three planes-lens, image, and subject-esulting in exceptional image clarity and depth of field [1]. While Pentacam® shows high intra-device precision, it has limitations with inter-device repeatability when compared to other tomography systems such as the Galilei and Orbscan II [2].

Pentacam® provides a detailed view of the anterior eye segment, making it indispensable in clinical scenarios including patient assessments, rapid screenings, and corneal evaluations [3, 4]. It measures parameters such as anterior chamber depth (ACD), anterior chamber angle (ACA), and anterior chamber volume (ACV), and produces pachymetry, elevation, and corneal densitometry maps (Figure 1. Graphical Abstract). Additionally, it generates comprehensive four-map refractive displays-covering anterior sagittal curvature, posterior elevation (PE), and pachymetry maps-which are essential for diagnosing conditions like keratoconus (KC) and subclinical keratoconus (SKC) [5, 6]. Diagnostic patterns, including the symmetric bowtie (suggestive of regular astigmatism) and more irregular shapes (like skewed hourglass patterns or tongue-like extensions), assist clinicians in recognizing abnormalities in corneal curvature and elevation [3].

his review will evaluate the diagnostic capabilities of Pentacam® indices, with an emphasis on identifying KC and SKC using key topographic and pachymetric parameters, such as the Belin-Ambrosio Enhanced Ectasia Display (BAD-D), Ambrósio relational thickness (ART), pachymetric progression index (PPI), and central corneal thickness (CCT).

Methods

The Pentacam® system employs a combination of Scheimpflug imaging and a 14-mm monochromatic slit lighting system to produce high-resolution images of the anterior segment of the eye [1, 7, 8]. By measuring parameters like ACD, ACA, and ACV simultaneously, it provides valuable data for diagnosing conditions such as KC and SKC [9-11]. The device's imaging capabilities are customizable, with suggested settings that include:

- Best-fit sphere (BFS) of either 8 mm or 9 mm for elevation maps,
- American-style cool scale,

- Step widths of 10 μm for pachymetry maps, 1 diopter (D) for topography maps, and 2.5 μm for elevation maps [3, 12, 13].

These settings enable the creation of detailed four-map refractive displays that give a comprehensive view of corneal parameters. The integration of anterior sagittal curvature, pachymetry, and posterior elevation maps allows for early detection of ectasia or corneal irregularities [14, 15]. Additionally, Pentacam® provides several quality metrics for its measurements, including:

- Q-value: Normal values range from-1 to 0, indicating a spherical or slightly prolate cornea; values above 0 suggest an oblate cornea, while values below-1 point to a hyperprolate cornea.
- Pupil center: Normal displacement ("x" value) is less than 200 μm, which is vital for evaluating angle kappa and ensuring precise IOL positioning during refractive surgeries [4, 16-18].

Diagnostic accuracy is further improved by the inclusion of schematic patterns, such as the symmetric bowtie (indicative of regular astigmatism) and the skewed hourglass pattern (observed in KC) [19, 20]. With these advanced settings and parameters, Pentacam® serves as a powerful tool for both preoperative evaluations and postoperative monitoring of patients with KC, SKC, and other corneal disorders.

Results

The Pentacam® system analyzes and calculates various parameters, including topographic, tomographic, and pachymetric measurements, producing a wealth of data that can be applied in numerous clinical situations. Among the topographic parameters it evaluates are the index of surface variance (ISV), index of vertical asymmetry (IVA), central keratoconus index (CKI), KI index of height asymmetry (IHA), index of height decentration (IHD), posterior elevation (PE), and minimal sagittal curvature (Rmin) [21-23].

y measuring both anterior and posterior elevations, Pentacam® creates PE maps based on a standard reference shape, such as the BFS or best-fit toric ellipsoid (BFTE). This method eliminates the steepening effect caused by the 3.5-mm area around the cornea's thinnest point, making it easier to detect any areas of protrusion [24, 25]. These elevation readings correspond to the Amsler-Krumeich severity index,[26] with ophthalmologists considering PE data to be a reliable indicator for identifying subtle KC changes [27, 28]. However, its ability to accurately detect SKC remains uncertain, so it is typically used alongside other parameters.

Like PE, other topographic indices-such as anterior elevation, CKI (the ratio of the mean curvature radius between a peripheral Placido ring and the central ring), KI (the curvature ratio between the upper and lower corneal segments), and IHA-are effective for distinguishing clinical KC from normal eyes [21, 22]. However, these indices are less reliable for differentiating SKC from healthy eyes, so caution is needed when using them independently for SKC detection, often requiring combination with other metrics [23]. Comparisons among Pentacam® indices show that KI tends to outperform CKI in diagnostic accuracy,[27] though some research suggests that KI is not as reliable as other Pentacam® indices [29]. Additionally, Rmin, which represents the maximum anterior curvature, has proven insufficient when used alone to diagnose KC or SKC [22].

In contrast, certain Pentacam® topographic indices have shown promising results for detecting both KC and SKC. The ISV, which is significantly elevated in individuals with irregular astigmatism, has been effective not only for identifying KC and SKC but also for monitoring disease progression [27, 30, 31]. Additionally, the IHD, which evaluates vertical centration using Fourier analysis, has demonstrated the ability to differentiate between SKC and unilateral KC, although its reliability in detecting SKC has been questioned in some studies, indicating a need for further validation [22, 32]. The IVA, which assesses symmetry in curvature relative to the horizontal meridian, is another useful metric for diagnosing both clinical and subclinical KC, [30, 33, 34] and is regarded as the second most accurate Pentacam® index for identifying KC [27, 35]. Some research even suggests that IVA may outperform certain pachymetric indices when distinguishing unilateral KC [22].

The evaluation of anterior sagittal curvature maps focuses on measurements like K1 (minimum curvature) and K2 (maximum curvature). In healthy eyes, the difference between K1 and K2 should be less than 1 diopter (D), while the mean curvature (Km) offers an average measurement for additional analysis. The normal differences between inferior-superior (I-S) and superior-inferior (S-I) measurements within the 5-mm central zone should be under 2.5 D, with abnormal values suggesting ectasia or KC progression [36-38].

Pentacam®'s pachymetry maps, generated with a step width of 10 μm, are highly accurate and reliable. In normal eyes, these maps typically appear concentric, whereas abnormal shapes, such as bell or dome configurations, signal corneal thinning, commonly seen in conditions like pellucid marginal degeneration (PMD) or keratoglobus [39, 40]. Moreover, the relative pachymetry map compares the patient's corneal thickness to a normative map, with minor deviations indicating normality and larger deviations (>-8%) pointing to potential abnormalities such as ectasia or other corneal disorders [41, 42].

Pentacam®'s pachymetric indices provide clinicians with the ability to monitor changes in corneal thickness, especially across the entire 360-degree circumference of the cornea [9, 43]. These indices include PPI (minimum, maximum, and average values), ART (minimum, maximum, and average values), BAD_D, central corneal thickness (CCT), Pentacam® random forest index (PRFI), and thinnest corneal thickness (TCT), all of which are essential for assessing the severity of KC. Many of these indices are considered reliable for evaluating both clinical and subclinical KC [9]. The data collected by Pentacam® supports the ABCD classification system, which incorporates the following components:

A. Anterior curvature: Curvature measurements taken within a 3-mm area surrounding the thinnest point of the cornea.

B. Posterior curvature: Posterior curvature readings from the

same 3-mm area.

C. Thinnest pachymetry: Measurement of the cornea's minimum thickness.

D. Best corrected distance visual acuity (BCVA): The highest visual acuity achievable with corrective lenses [44, 45].

This system overcomes the limitations of the Amsler-Krumeich and KSI classification methods, particularly by including posterior elevation data at the cornea's thinnest point, and is also effective in detecting unilateral KC [46].

The PPI measures corneal thickness variations over 360 degrees, with an average value of 0.13, a maximum of 0.85, and a minimum of 0.58 [43]. Normal PPI values range from 0.8 to 1.1, with values above 1.2 indicating ectasia, while values below 0.8 suggest corneal edema or other diseases [47, 48]. PPI is considered more dependable than single-point thickness measurements for diagnosing both KC and SKC, although some studies report that its area under the curve (AUC) is less than 0.90 [22, 32].

With the maximum accuracy at a cut-off value between 300 and 400 µm, ART is a more recent diagnostic technique for KC. It determines the ratio between the thinnest corneal point and PPI, with the following cut-off values:

- ART Min: Cut-off of 424 µm,
- ART Max: Cut-off of 412 µm [19, 49, 50].

These cut-off values are highly predictive of ectasia risk, with lower values correlating to a higher likelihood of ectatic progression. ART is particularly valuable for early detection of corneal ectatic disorders; however, its reliability in diagnosing SKC remains controversial, as the diagnostic results have been inconsistent [51, 52].

The BAD_D index is a multivariate metric that combines nine different indices to provide a comprehensive assessment of the cornea. It utilizes pachymetric and curvature data to evaluate the normality of several parameters, including anterior elevation deviation (Df), posterior elevation deviation (Db), pachymetric progression deviation (Dp), deviation of the cornea's thinnest point (Dt), and relational thickness deviation (Da). The average values from a healthy population are set at zero, allowing for the calculation of standard deviations (SD) to determine disease presence. The software provides a regression analysis, which is color-coded to aid in clinical interpretation:

- White: < 1.6 SD (normal),
- Yellow: 1.6-2.6 SD (suspected KC),
- Red: > 2.6 SD (clinical KC) [9, 29, 33, 53, 54].

This system has demonstrated high accuracy in detecting KC, and some studies indicate that it may also be useful for monitoring postoperative changes, such as after corneal cross-linking (CXL). Although BAD_D has proven to be highly accurate for both clinical KC and SKC diagnosis, further studies are required to confirm its effectiveness in unilateral KC cases [22].

One of the important diagnostic features offered by Pentacam® is the Corneal Thickness Spatial Profile (CTSP) [55]. This index measures corneal thickness across the entire surface, following a normative black dotted curve. Deviations from this curve help assess corneal health, with irregularities in the CTSP curve suggesting ectatic changes or corneal thinning. While a normal CTSP follows a smooth curve, an abnormal one shows deviations, such as an S-shape, indicating either thicker or thinner corneal areas than expected [4, 24].

The Percentage Thickness Increase (PTI) further enhances this evaluation by analyzing the relative changes in corneal thickness. Normal PTI values fall between 0.8 and 1.1, with values above 1.1 indicating ectatic changes, and values below 0.8 suggesting corneal edema or other issues. Both CTSP and PTI are critical in detecting early ectasia, where small changes in corneal thickness often serve as the first signs of pathology [56, 57].

CCT has been an essential diagnostic measure for over three decades, especially in cases of topographic asymmetry. While CCT is a reliable tool for screening KC, its utility in postoperative monitoring and SKC diagnosis is more limited [58]. PRFI was developed as a sensitive tool for detecting ectasia by utilizing artificial intelligence (AI) to analyze corneal data. PRFI combines several factors, including integrated radius, A1 velocity, and deflection amplitude, to improve diagnostic sensitivity. With a cut-off value of 0.216, PRFI achieves a sensitivity of 98.8% and a specificity of 94.2% [3, 10, 14, 59]. However, it misdiagnosed 20% of SKC cases, making it less effective than the BAD_D index [60, 61]. Despite this limitation, PRFI shows promise as an advancement in corneal diagnostics by integrating AI with conventional imaging methods [56, 62]. TCT is another reliable measure for screening KC at different stages, although its AUC is typically lower than that of other Pentacam® parameters [9, 52, 63].

Discussion

Pentacam® is instrumental in postoperative evaluations of corneal and refractive surgeries, including Laser-Assisted in Situ Keratomileusis (LASIK), Photorefractive Keratectomy (PRK), and corneal grafts. Its detailed four-map refractive display enables clinicians to assess surgical outcomes and identify potential complications such as ectasia or irregular astigmatism [3, 12, 15]. In post-LASIK patients, Pentacam® assesses ACD and ACA to ensure corneal stability following surgery. For corneal graft follow-ups, it offers comprehensive pachymetry and elevation maps, which are useful for monitoring graft integrity and identifying any complications [42].

In post-refractive surgery cases, Pentacam®'s Holladay report is especially helpful. It produces six maps, including topography, axial and tangential curvature maps, and anterior elevation maps [50]. These maps are essential for monitoring corneal health and calculating IOL power in patients with irregular or surgically modified corneas. The back/front radius of curvature (ROC) in the Holladay report provides an accurate view of corneal power distribution, which is critical for post-surgery IOL power

calculations [3, 4].

Pentacam® also aids in detecting forme fruste keratoconus (FFKC), a subclinical form of the disease that can go undetected by conventional imaging methods [55]. The combination of BAD-D and PRFI in these cases offers early indicators of ectatic changes, allowing for earlier intervention [20].

Pentacam® is valuable in evaluating both pre- and post-operative suitability for phakic IOL (pIOL) implantation. Preoperatively, the device assesses crucial factors, such as:

- ACD greater than 3mm,
- ACA greater than 30 degrees,
- Mesopic pupil size relative to the pIOL optic,
- Endothelial cell count (ECC) according to the patient's age.

These criteria ensure the cornea's suitability for pIOL implantation, minimizing the risk of complications like endothelial cell loss or improper IOL placement. [3, 4, 10] Postoperatively, Pentacam® monitors parameters like angle, ACD, and ACV to confirm pIOL stability and ensure the patient does not experience complications such as iris configuration changes or corneal decompensation.

Beyond common conditions like keratoconus, Pentacam® is indispensable for diagnosing rarer corneal disorders such as PMD and keratoglobus. In PMD cases, its pachymetry map often shows a bell-shaped thinning pattern in the inferior cornea, which can be mistaken for keratoconus. Pentacam®'s precise corneal thickness measurements enable accurate differentiation between PMD and other ectatic disorders. In keratoglobus, the pachymetry maps reveal generalized thinning in a globus pattern that extends to the corneal limbus [39, 40]. These cases require careful monitoring and, in some instances, surgical intervention. Pentacam® equips clinicians with the tools to track disease progression and evaluate the necessity of corneal grafting or other treatments.

While Pentacam® is highly effective for diagnosing KC, it faces challenges when it comes to detecting SKC. Despite its advanced imaging capabilities, the device has limitations in terms of inter-device repeatability. Although it performs well within a single device, consistency across different devices and models is less reliable, particularly in measurements like posterior elevation and TCT [14, 42, 64, 65]. This inconsistency affects the comparability of results between clinics using different Pentacam® models.

Zernike polynomial modeling has shown promise in distinguishing SKC from normal cases, but this conclusion is based on limited research, and further studies are necessary to validate its effectiveness for diagnosing SKC [66]. One of the main issues in assessing the accuracy of any index for differentiating SKC from normal eyes is the inconsistent definition of SKC across studies. Terms such as FFKC, SCK, borderline, suspect, and early-stage KC are often used interchangeably, making direct comparisons difficult. Additionally, variations in participant selection criteria across studies further complicate the interpretation of SKC results. For example, while indices like PPI and BAD-D show high diagnostic accuracy for clinical KC, their performance is less consistent for SKC detection [26, 27].

Certain topographic indices, like CKI, perform well in distinguishing clinical KC from normal eyes, but their effectiveness diminishes when used to differentiate SKC from healthy corneas [6, 7, 8]. Similarly, indices such as Rmin and IHD exhibit reduced diagnostic accuracy in SKC cases, making early detection more difficult [7].

A significant challenge in using Pentacam® is the variability in diagnostic criteria across studies and clinical settings [67, 68]. For instance, differences in BAD-D cut-off values or in the interpretation of PTI and CTSP can lead to inconsistent diagnoses. To enhance diagnostic consistency, there is a need to standardize criteria for all Pentacam® parameters, especially in the early detection of ectasia.

Conclusion

Pentacam® remains a valuable tool in the diagnosis and management of KC and SKC through its comprehensive corneal imaging capabilities. While indices such as BAD-D, ART, and PPI show high diagnostic accuracy for clinical KC, the detection of SKC remains a challenge due to variability in diagnostic criteria. The integration of advanced techniques like the PRFI and AI holds promise for improving diagnostic reliability, especially for SKC. Future research should focus on standardizing diagnostic protocols and further refining these indices to enhance accuracy and inter-device reliability.

Acknowledgements

The authors would like to acknowledge Mr. Hamidreza Nematy for his invaluable assistance with the writing of this manuscript.

Financial Support

None.

Conflict of Interest

The authors declare that they have no conflicts of interest.

References

1. Ambrosio R Jr (2013) Scheimpflug imaging for laser refractive surgery. Curr Opin Ophthalmol, 24(4): 310-320.
2. Hernández-Camarena JC (2014) Repeatability, reproducibility, and agreement between three different Scheimpflug systems in measuring corneal and anterior segment biometry. Journal of Refractive Surgery. 30(9): 616-621.
3. Niazi S (2023) Keratoconus Diagnosis: From Fundamentals to Artificial Intelligence: A Systematic Narrative Review. Diagnostics (Basel) 13(16): 2715.
4. Mohammadpour M, Z Heidari (2021) Pentacam, in Diagnostics in Ocular Imaging: 65-162.
5. Asam JS (2019) Anterior Segment OCT, in High Resolution Imaging in Microscopy and Ophthalmology: New Frontiers in Biomedical Optics. 285-299.
6. Safarzadeh M and N Nasiri (2016) Anterior segment characteristics in normal and keratoconus eyes evaluated with a combined Scheimpflug/Placido corneal imaging device. J Curr Ophthalmol 28(3): 106-111.

7. Ambrosio R Jr (2017) Integration of Scheimpflug-Based Corneal Tomography and Biomechanical Assessments for Enhancing Ectasia Detection. J Refract Surg 33(7): 434-443.
8. Steinberg J (2015) Screening for Keratoconus with New Dynamic Biomechanical In Vivo Scheimpflug Analyses. Cornea 34(11): 1404-1412.
9. Motlagh MN (2019) Pentacam® Corneal Tomography for Screening of Refractive Surgery Candidates: A Review of the Literature, Part I. Med Hypothesis Discov Innov Ophthalmol 8(3): 177-203.
10. Afifah A (2024) Artificial intelligence as diagnostic modality for keratoconus: A systematic review and meta-analysis. J Taibah Univ Med Sci 19(2): 296-303.
11. Atalay E, O Ozalp and N Yildirim (2021) Advances in the diagnosis and treatment of keratoconus. Ther Adv Ophthalmol 13: 25158414211012796.
12. Hashemi H (2024) Comparison of different corneal imaging modalities using artificial intelligence for diagnosis of keratoconus: a systematic review and meta-analysis. Graefes Arch Clin Exp Ophthalmol 262(4): 1017-1039.
13. Issarti I (2019) Computer aided diagnosis for suspect keratoconus detection. Comput Biol Med 109: 33-42.
14. Ambrosio R Jr (2023) Optimized Artificial Intelligence for Enhanced Ectasia Detection Using Scheimpflug-Based Corneal Tomography and Biomechanical Data. Am J Ophthalmol 251: 126-142.
15. Yang K (2020) Evaluation of new Corvis ST parameters in normal, Post-LASIK, Post-LASIK keratectasia and keratoconus eyes. Sci Rep 10(1): 5676.
16. Mohammadpour M (2022) Comparison of Artificial Intelligence-Based Machine Learning Classifiers for Early Detection of Keratoconus. Eur J Ophthalmol 32(3): 1352-1360.
17. Armstrong BK (2021) Screening for Keratoconus in a High-Risk Adolescent Population. Ophthalmic Epidemiol 28(3): 191-197.
18. Ruiz Hidalgo I (2017) Validation of an Objective Keratoconus Detection System Implemented in a Scheimpflug Tomographer and Comparison with Other Methods. Cornea 36(6): 689-695.
19. Owusu S (2023) Scheimpflug-Derived Keratometric, Pachymetric and Pachymetric Progression Indices in the Diagnosis of Keratoconus: A Systematic Review and Meta-Analysis. Clin Ophthalmol 17: 3941-3964.
20. Henriquez MA, M Hadid and L Izquierdo Jr (2020) A Systematic Review of Subclinical Keratoconus and Forme Fruste Keratoconus. J Refract Surg 36(4): 270-279.
21. Du XL, M Chen and LX Xie (2015) Correlation of basic indicators with stages of keratoconus assessed by Pentacam tomography. Int J Ophthalmol 8(6): 1136-1140.
22. Bae GH (2014) Corneal topographic and tomographic analysis of fellow eyes in unilateral keratoconus patients using Pentacam. Am J Ophthalmol 157(1): 103-109e1.
23. de Sanctis U (2008) Sensitivity and specificity of posterior corneal elevation measured by Pentacam in discriminating keratoconus/subclinical keratoconus. Ophthalmology 115(9): 1534-1539.
24. Hashem AO (2023) Diagnostic accuracy of different keratoconus detection indices of pentacam in paediatric eyes. Eye (Lond) 37(6): 1130-1138.
25. Kovacs I (2011) The role of reference body selection in calculating posterior corneal elevation and prediction of keratoconus using rotating Scheimpflug camera. Acta Ophthalmol 89(3): e251-256.
26. Ishii R (2012) Correlation of corneal elevation with severity of keratoconus by means of anterior and posterior topographic analysis. Cornea 31(3): 253-258.
27. Orucoglu F and E Toker (2015) Comparative analysis of anterior segment parameters in normal and keratoconus eyes generated by scheimpflug tomography. J Ophthalmol: 925414.
28. Jafarinasab M R (2015) Sensitivity and specificity of posterior and anterior corneal elevation measured by orbscan in diagnosis of clinical and subclinical keratoconus. J Ophthalmic Vis Res 10(1): 10-5.
29. Chan T C (2018) Comparison of corneal dynamic parameters and tomographic measurements using Scheimpflug imaging in keratoconus. Br J Ophthalmol 102(1): 42-47.
30. Shetty R (2014) Repeatability and agreement of three Scheimpflug-based imaging systems for measuring anterior segment parameters in keratoconus. Invest Ophthalmol Vis Sci 55(8): 5263-5268.
31. John A K and G Asimellis (2013) Revisiting keratoconus diagnosis and progression classification based on evaluation of corneal asymmetry indices, derived from Scheimpflug imaging in keratoconic and suspect cases. Clinical Ophthalmology 7: 1539-1548.
32. Huseynli S and F Abdulaliyeva (2018) Evaluation of Scheimpflug Tomography Parameters in Subclinical Keratoconus, Clinical Keratoconus and Normal Caucasian Eyes. Turk J Ophthalmol 48(3): 99-108.
33. Hashemi H (2016) Pentacam top indices for diagnosing subclinical and definite keratoconus. J Curr Ophthalmol 28(1): 21-26.
34. Arbelaez M C (2012) Use of a support vector machine for keratoconus and subclinical keratoconus detection by topographic and tomographic data. Ophthalmology 119(11): 2231-2238.
35. Belin MW and SS Khachikian (2009) An introduction to understanding elevation-based topography: how elevation data are displayed-a review. Clinical & experimental ophthalmology 37(1): 14-29.
36. Deshmukh R (2023) Management of keratoconus: an updated review. Front Med (Lausanne) 10: 1212314.
37. Shajari M (2019) Evaluation of keratoconus progression. Br J Ophthalmol 103(4): 551-557.
38. Martinez-Abad A and DP Pinero (2017) New perspectives on the detection and progression of keratoconus. J Cataract Refract Surg 43(9): 1213-1227.
39. Levy A (2022) Corneal Epithelial Thickness Mapping in the Diagnosis of Ocular Surface Disorders Involving the Corneal Epithelium: A Comparative Study. Cornea 41(11): 1353-1361.
40. Al-Timemy A H (2021) A Hybrid Deep Learning Construct for Detecting Keratoconus from Corneal Maps. Transl Vis Sci Technol 10(14): 16.
41. Krachmer J H, R S Feder and M W Belin (1984) Keratoconus and related noninflammatory corneal thinning disorders. Surv Ophthalmol 28(4): 293-322.
42. Shehata A E M (2020) The Correlation between Corneal Findings and Disease Severity in Keratoconus per Scheimpflug Corneal Tomography. J Ophthalmol: 4130643.
43. Ambrósio R (2013) Enhanced screening for ectasia susceptibility among refractive candidates: the role of corneal tomography and biomechanics. Current Ophthalmology Reports 1(1): 28-38.
44. Belin M W and J K Duncan (2016) Keratoconus: The ABCD Grading System. Klin Monbl Augenheilkd 233(6): 701-707.
45. Belin M (2015) A new tomographic method of staging/classifying keratoconus: the ABCD grading system. Int J Kerat Ect Cor Dis 4(3): 55-63.
46. Imbornoni L M (2017) Long-Term Tomographic Evaluation of Unilateral Keratoconus. Cornea 36(11): 1316-1324.
47. Fuentes E (2015) Anatomic Predictive Factors of Acute Corneal Hydrops in Keratoconus: An Optical Coherence Tomography Study. Ophthalmology 122(8): 1653-1659.

48. Siganos CS (2010) Changing indications for penetrating keratoplasty in Greece, 1982-2006: a multicenter study. Cornea 29(4): 372-374.

49. Vinciguerra R (2016) Detection of Keratoconus with a New Biomechanical Index. J Refract Surg 32(12): 803-810.

50. Ambrosio R Jr (2011) Novel pachymetric parameters based on corneal tomography for diagnosing keratoconus. J Refract Surg 27(10): 753-758.

51. Muftuoglu O (2015) Comparison of multimetric D index with keratometric, pachymetric, and posterior elevation parameters in diagnosing subclinical keratoconus in fellow eyes of asymmetric keratoconus patients. J Cataract Refract Surg 41(3): 557-565.

52. Sedaghat M R (2018) Diagnostic Ability of Corneal Shape and Biomechanical Parameters for Detecting Frank Keratoconus. Cornea 37(8): 1025-1034.

53. Mohammadpour M (2020) Diagnostics in Ocular Imaging: Cornea, Retina, Glaucoma and Orbit. Springer Nature.

54. Moshirfar M (2019) Galilei Corneal Tomography for Screening of Refractive Surgery Candidates: A Review of the Literature, Part II. Med Hypothesis Discov Innov Ophthalmol 8(3): 204-218.

55. Saad A and D Gatinel (2010) Topographic and tomographic properties of forme fruste keratoconus corneas. Invest Ophthalmol Vis Sci 51(11): 5546-5555.

56. Abdelmotaal H (2020) Classification of Color-Coded Scheimpflug Camera Corneal Tomography Images Using Deep Learning. Transl Vis Sci Technol 9(13): 30.

57. Sella R (2019) Repeatability and Reproducibility of Corneal Epithelial Thickness Mapping with Spectral-Domain Optical Coherence Tomography in Normal and Diseased Cornea Eyes. Am J Ophthalmol 197: 88-97.

58. Guarnieri FA (2015) Introduction: Corneal Biomechanics and Refractive Surgery, in Corneal Biomechanics and Refractive Surgery. Springer: 1-6.

59. Niazi S (2023) Association of 2 Lysyl Oxidase Gene Single Nucleotide Polymorphisms with Keratoconus: A Nationwide Registration Study. Ophthalmol Sci 3(2): 100247.

60. Lopes B T (2018) Enhanced Tomographic Assessment to Detect Corneal Ectasia Based on Artificial Intelligence. Am J Ophthalmol 195: 223-232.

61. Haddad J (2017) First clinical impressions on the integrated corneal tomography and corneal deformation with scheimpflug imaging. International Journal of Keratoconus and Ectatic Corneal Diseases 6: 101-109.

62. Abdelmotaal H (2021) Pix2pix Conditional Generative Adversarial Networks for Scheimpflug Camera Color-Coded Corneal Tomography Image Generation. Transl Vis Sci Technol 10(7): 21.

63. Demir S (2013) Mapping corneal thickness using dual-scheimpflug imaging at different stages of keratoconus. Cornea 32(11): 1470-1474.

64. Kang L, D Ballouz and M A Woodward (2022) Artificial intelligence and corneal diseases. Curr Opin Ophthalmol 33(5): 407-417.

65. Herber R, L E Pillunat and F Raiskup (2021) Development of a classification system based on corneal biomechanical properties using artificial intelligence predicting keratoconus severity. Eye Vis (Lond) 8(1): 21.

66. Xu Z (2017) Characteristic of entire corneal topography and tomography for the detection of sub-clinical keratoconus with Zernike polynomials using Pentacam. Sci Rep 7(1): 16486.

67. Flockerzi E (2022) Combined biomechanical and tomographic keratoconus staging: Adding a biomechanical parameter to the ABCD keratoconus staging system. Acta Ophthalmol 100(5): e1135-e1142.

68. Maile H (2021) Machine Learning Algorithms to Detect Subclinical Keratoconus: Systematic Review. JMIR Med Inform 9(12): e27363.